Aperture efficiency of the 40m radiotelescope at C-band, X-band, K-band, Q-band and W-band

M. Rodríguez, M. Gómez-Garrido, P. de Vicente

Informe Técnico IT-OAN 2017-12

Revision history

Version	Date	Author	Updates
1.0	10-01-2017	M. Rodríguez, M. Gómez-Garrido P. de Vicente	First version

Contents

1 Introduction

Efficiency curves provide valuable information about the state of the radiotelescope. Periodic observations to estimate it at different observing frequencies are convenient and useful to detect any problem in the primary reflector or any other element along the ray path.

The aperture efficiency (we will call it simply efficiency) for the 40m Yebes radio telescope is given by the expression:

$$\eta_a = 2.197 \, \frac{T_a^* \, C_S \, \eta_f}{S[Jy]} \, , \tag{1}$$

where T_a^* is the antenna temperature (expressed in kelvin), η_f is the forward efficiency, C_S is the deconvolution function of the beam and $S[Jy]$ is the source flux in Jansky. The value 2.197 comes from $2K_B/A$, where K_B is the Boltzmann's constant and A is the area of the 40 m radiotelescope.

The efficiency depends on frequency and elevation, and both dependencies arise from deformations of the reflectors or their supporting structures.

Usually, the dependency of the efficiency on elevation is referred to as gain, and it is normalized to 1 at its maximum and the word "efficiency" is reserved only to that maximum. Therefore, the aperture efficiency would be:

$$\eta_a(el) = Efficiency * gain(el) \tag{2}$$

The dependency of the gain on elevation come basically from the gravitational deformation of the structure. The frequency dependency is a consequence of the scale of the deformations compared to the wavelength. For antennas with an homological design, like to 40 m radiolescope, the dependency with elevation should be weak.

In addition to the dependencies on frequency and elevation, the efficiency presents seasonality. The different temperatures along the year cause deformations on the structure that might be related to astigmatism (Visus, de Vicente and Pérez, 2013) . Hence, observations to determine the efficiency should take place at several moments of the year.

The efficiency should be maximum to attain high quality astronomical observations. In order to properly parametrize changes in this magnitude, comparison of its values at different frequencies, in a wide range of elevations and at different moments of the year should be done. This report only shows the results of observations from the 2016-2017 winter season at Yebes.

2 Efficiency observations

Observations were made using the continuum backend IRAM-Detector, *IDET*, from December 2016 to January 2017 (see de Vicente et al. 2014). Due to the variability

of the efficiency as a function of frequency, four frequency ranges were tuned [C-band (6.6 GHz); X-band (8.4 GHz); K-band (22.3 GHz); Q-band (45.5 GHz)]. Additionally, on April 2017 some observations were carried out using the W-band receiver (86.2 GHz). All observations were done in good weather conditions. The nocturnal and diurnal observations were mixed and the results are averaged.

To achieve the best efficiency curves, astronomical sources with a well-known and high continuum flux must be selected. In some cases fluxes were obtained from precise observations from other observatories. The observed sources are listed in Table 1.

Source	C-Band	X-Band	K-Band	Q-Band	Type *
Venus ★			●	●	Planet
Jupiter				●	Planet
Saturn			●	●	Planet
Cas-A	●	●			SNR
Tau-A	●	●			SNR
Cyg-A	●	●			AGN
Vir-A	●	●			AGN
DR21			●	●	SFR
3C48	●	●			Quasar
3C84			●	●	Quasar
3C123	●	●			Quasar
3C138	●	●			Quasar
3C147	●	●			Quasar
3C196	●				Quasar
3C286	●	●			Quasar
3C295	●	●			Quasar
3C380	●	●			Quasar

Table 1: Observed sources and receivers used. Red dots represent problematic sources, due to their big angular size or their low flux. Types*. SNR: Supernova remmant; AGN: Active galactic nuclei; SFR: Star forming region. ★: Venus has also been observed with the W-band receiver.

Ideally, the flux of an amplitude calibrator should be constant in time. However, the flux is variable for the sources above (see Fuhrmann et al. 2016). The flux of planets can be easily computed assuming that they radiate as black bodies heated by the Sun. They are specially useful above 20 GHz. Below that frequency their brigthness is too low. The flux from quasars relies on observations from other telescopes.

3 Data analysis

Although Cas-A, Cyg-A, Tau-A, Vir-A and Jupiter were observed they were not taken into account in later calculations. The efficiency values obtained with the data from them were completely unlikely, since they were extraordinary high ($> 100\%$!).

We concluded that their big sizes cause the value of the deconvolution function to be very high when evaluated, resulting in large and unreal values of efficiency. The big size of this extense sources can be compared individually with other point sources. A continuum observation of a point source gives a gaussian whose FWHM is the approximately size of the antenna beam width. On the contrary, if the source is extended, the result is similar to a gaussian but in which the FWHM corresponds to the convolution of the antenna beam with the size of the source.

The size and flux of the source are two very important parameters and they are required for the analysis of each frequency range. On the one hand, planets are usual sources used for calibrating the instruments of the antenna and for determining the efficiency, because their fluxes and apparent sizes are precisely provided by models. In our case, we have used the software *ASTRO* from *GILDAS*.

On the other hand, for quasars we have calculated the fluxes using the equation:

$$\log S[Jy] = \sum_i a_i \left[\log(\nu_G[GHz])\right]^i , \tag{3}$$

where we have used the coefficients given in Perley & Butler [**?**] for several sources. However, for DR21 and 3C84 the necessary coefficients were not contained in these paper, so we had to search the fluxes of these sources in the database of the National Radio Astronomy Observatory (NRAO).

The apparent size for planets, dependent on the date and time of the observation, was obtained using *ASTRO*, and for all quasars we used the the parameters summarized in Field System file *flux.ctl*. The size of the source at a given frequency, θ_S, is necessary to calculate the deconvolution function, C_S, since it depends on θ_S through $x = \theta_S / 1.2\,\theta_b$, where θ_b is the beam of the radiotelescope. Depending on the ratio of θ_S to θ_b, it should be considered the disk or the gaussian expression of this function.

In order to calculate the efficiency of the antenna at different frequencies we have developed a set of scripts, available in *https://hercules.oan.es/redmine*. Each of these scripts executes a part of the process to achieve the final result. The programms require information about the frequency band of the observation as input. Information of the receiver is then searched in a catalogue specifically written for this purpose, as well as information about the observed sources in that frequency in other catalogue. Schmatically, the procedure looks as follows:

1. At first, programm *temperatures_pro.py* must be executed. This programm takes as input the .40m CLASS file. Firstly, it shows the first pointing image contained in the .40m file to allow us to select a window which will be applied to all images. Then, it will fit a baseline to each image and will make a fit to obtain the antenna temperature. The fitting data are saved in an output file.

2. The second step consists in the execution of the programm *efficiency_pro.py*. This takes as input the previous file containing the fitting data. The programm will ask us about the frequency band or sub-band which our data belong to. It is possible to give optional information as well, like the frequency of the observed line and the observation date (this is only used for the title of the plots). After this, the programm will show us the different sources that have been observed and will ask if there is any of them we do not want to consider.

Finally, it will display a graph with the efficiency values of the antenna as a function of the elevation of each of the considered sources. The values of elevation, aperture efficiency and observed source will be saved in a text file.

efficiency_pro.py reads two text files: *antenna_parameters.txt*, which contains information about each receiver. This information is necessary to calculate the efficiency. The other text file is *source_catalogue.txt*, which consists in a catalogue with source parameters in the observing frequency. We have developed the procedure in this way since we do not want, if possible, to re-write the code, at leastn if the problem is that any parameter of the antenna must be changed.

3. Lastly, if we consider it worth it, we will execute the programm *rescale_pro.py*. It reads the text file generated in step 2 and it will plot again the aperture efficiency vs. elevation graph, distinguishing each source with a different colour. Then, the programm will ask us if we would like to scale the plotted efficiencies with a planet, if there is any among the observed sources. If we decide to scale, the programm will plot the efficiencies of the non-planet sources scaled with respect to the planet choosen as reference (if there are more planets observed, they will be not scaled with respect to the reference one). In this graph the data corresponding to each source will be plotted in different colours as well. At last, a data file is generated, containing the elevations and the efficiencies, without distinguishing between sources. This last file could be used in the future to represent again the efficiency curve of the antenna in that frequency.

   The scaling is done by calculating, for a given source, the mean value of the efficiency obtained with it and then substracting this mean value to the one calculated with the reference planet. After that, it adds the calculated difference to each value of efficiency given by the considered source.

Despite of this procedure, we highly suggest to proceed at first as follows: if the number of pointing observations is not too high, it is recomendable to check every image and discard those with low quality (a new .40m file should be created, containing only the images with good quality). In any case, whether the amount of images is big as if it is small, it is necessary to plot the points (distinguishing between sources) and check if there are any of them that do not lay on the tendency (this can be done by executing *efficiency_pro.py*). If so, execute CLASS and find which image the outlier belongs to. If you do not want to create a new .40m file, which does not contain the image of the outlier, you can simply comment the corresponding line of data in the output file generated by *temperatures_pro.py*. Once you have detected all bad quality points and have commented their corresponding data lines, you can execute *efficiency_pro.py* normally.

4 Results

In the following images the obtained results of aperture efficiency are shown. The first one shows the absolute value of this magnitude, while the second image

represents the same curves, but they have been normalized for a better comparison.

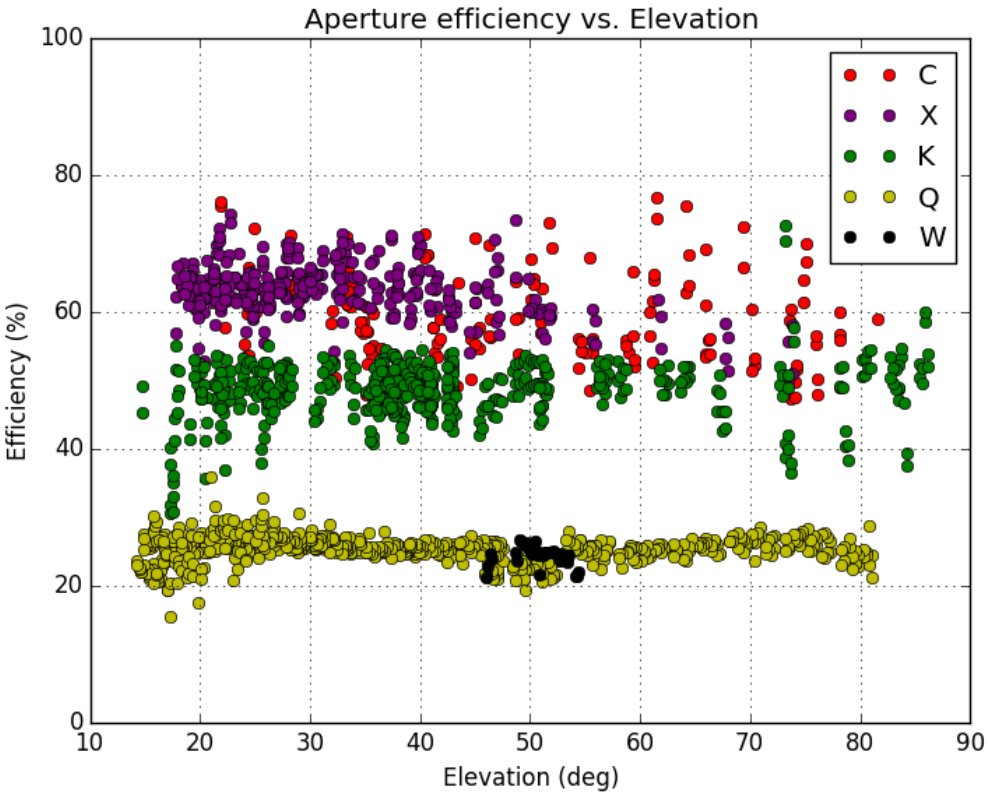

Figure 1: Efficiency curves of the different receivers employed.

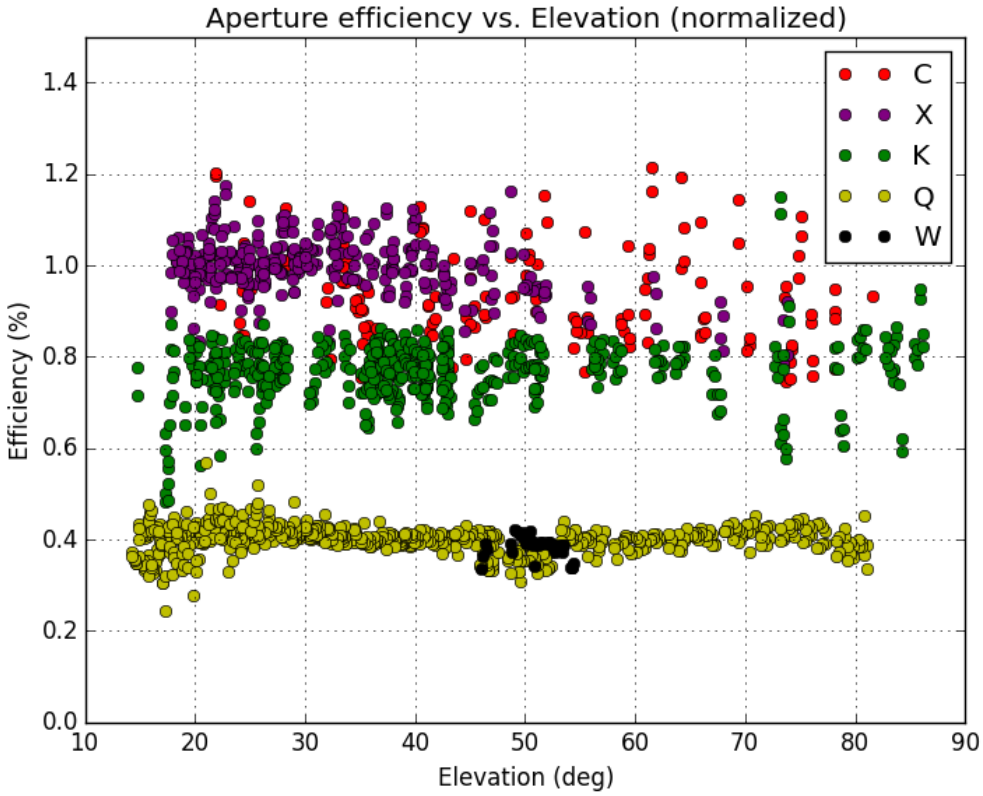

Figure 2: Normalized efficiency curves of the different receivers employed. They have been normalized by the highest value of the mean efficiency.

The normalization has been made by calculating the mean value of efficiency for each receiver and then dividing each point by the highest mean value found.

The plots shown above have been obtained following the procedure described in section 3. Since no planet has been observed with C-band and X-band receivers, it was not possible to scale with a planet the multiple curves obtained for each source. The points corresponding C-band, at both measured frequencies, present an important dispersion.

In addition, in the next figures we represent, separately for each frequency band, the dependency of the efficiency on the elevation together with three different fits: linear, sinusoidal and parabollic fits.

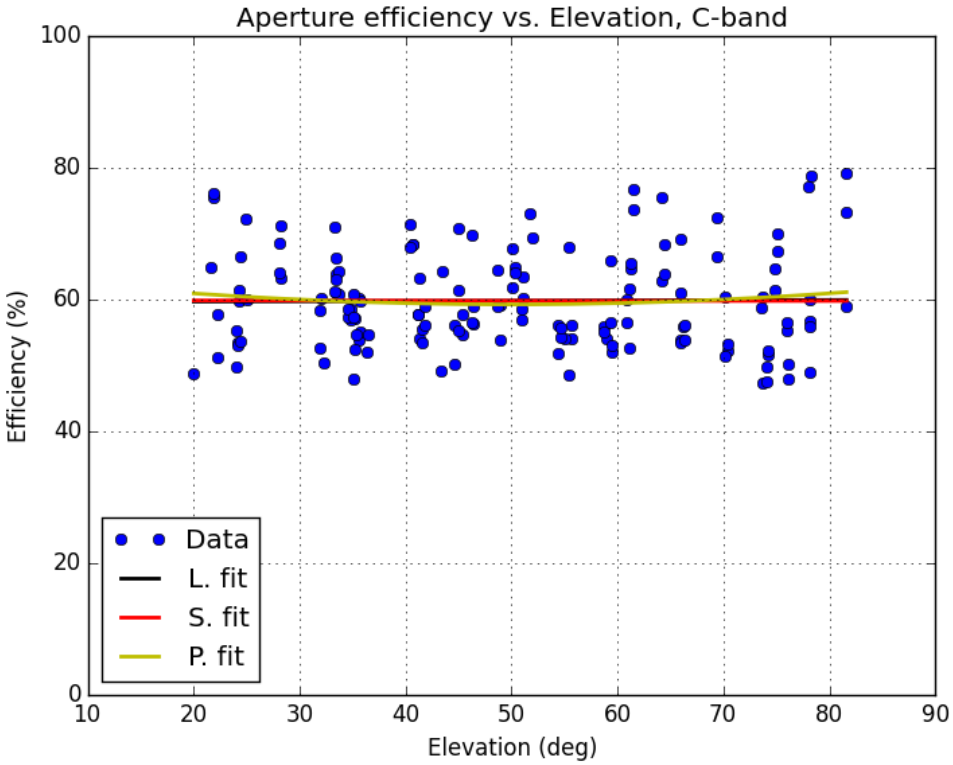

Figure 3: Dependency of the efficiency at C-band on the elevation, together with three fits: linear, sinusoidal and parabollic.

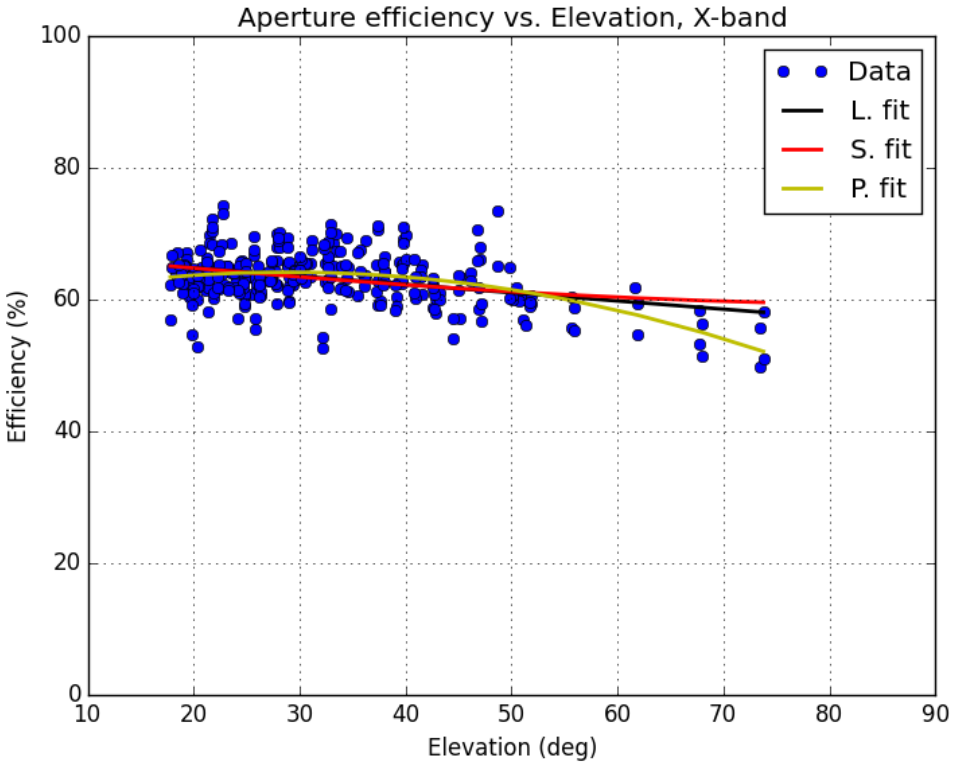

Figure 4: Dependency of the efficiency at X-band on the elevation, together with three fits: linear, sinusoidal and parabollic.

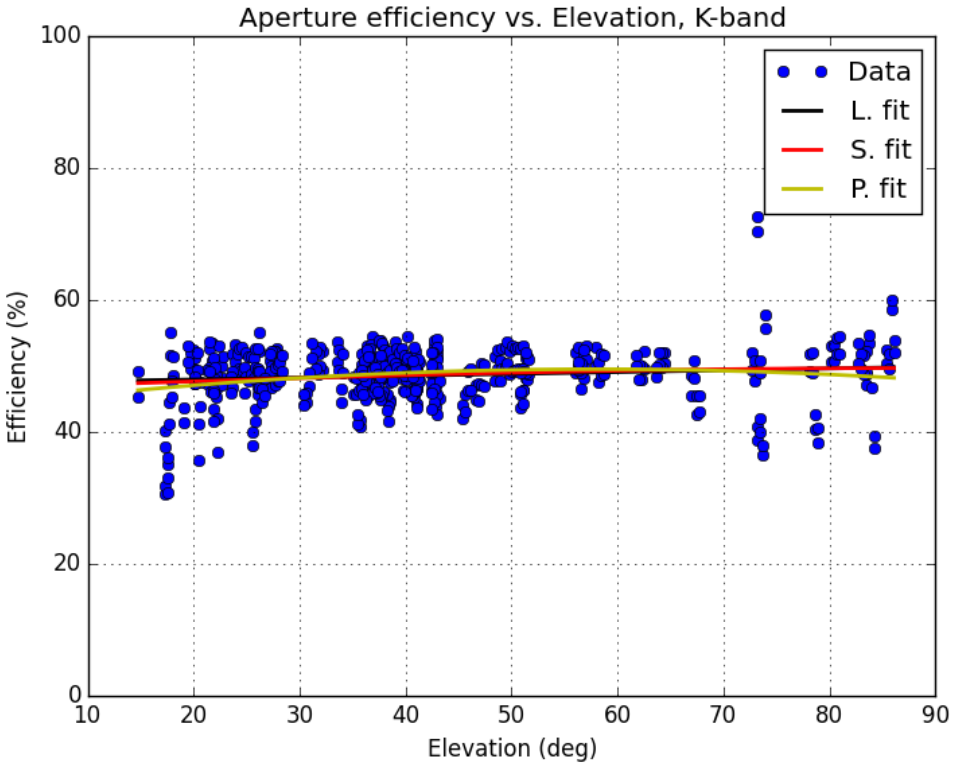

Figure 5: Dependency of the efficiency at K-band on the elevation, together with three fits: linear, sinusoidal and parabollic.

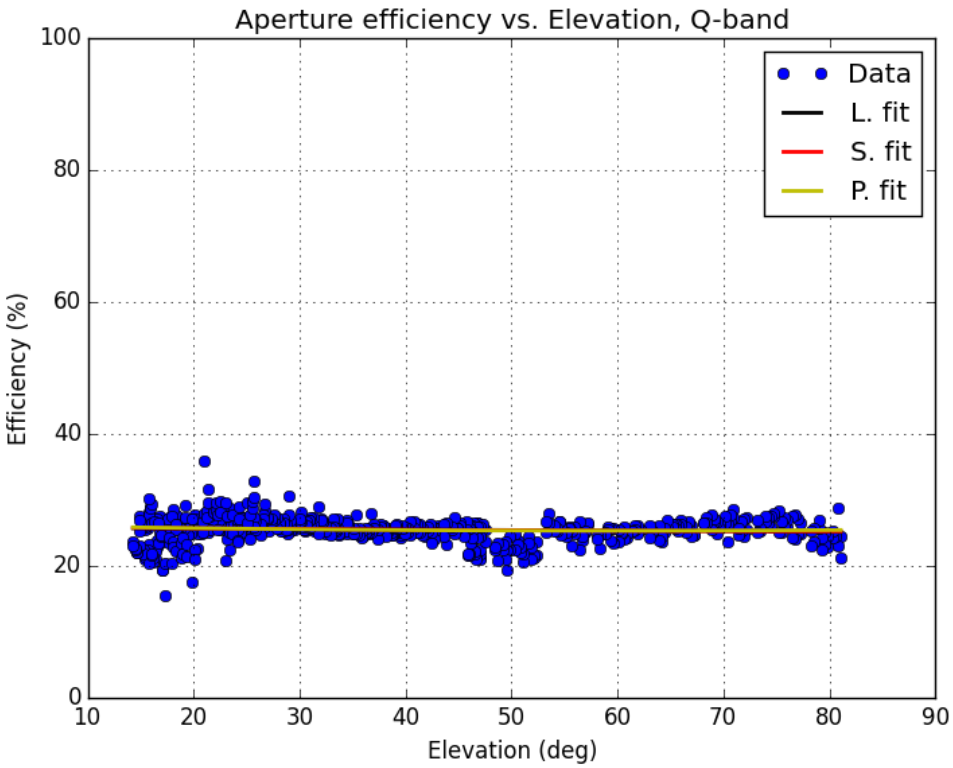

Figure 6: Dependency of the efficiency at Q-band on the elevation, together with three fits: linear, sinusoidal and parabollic.

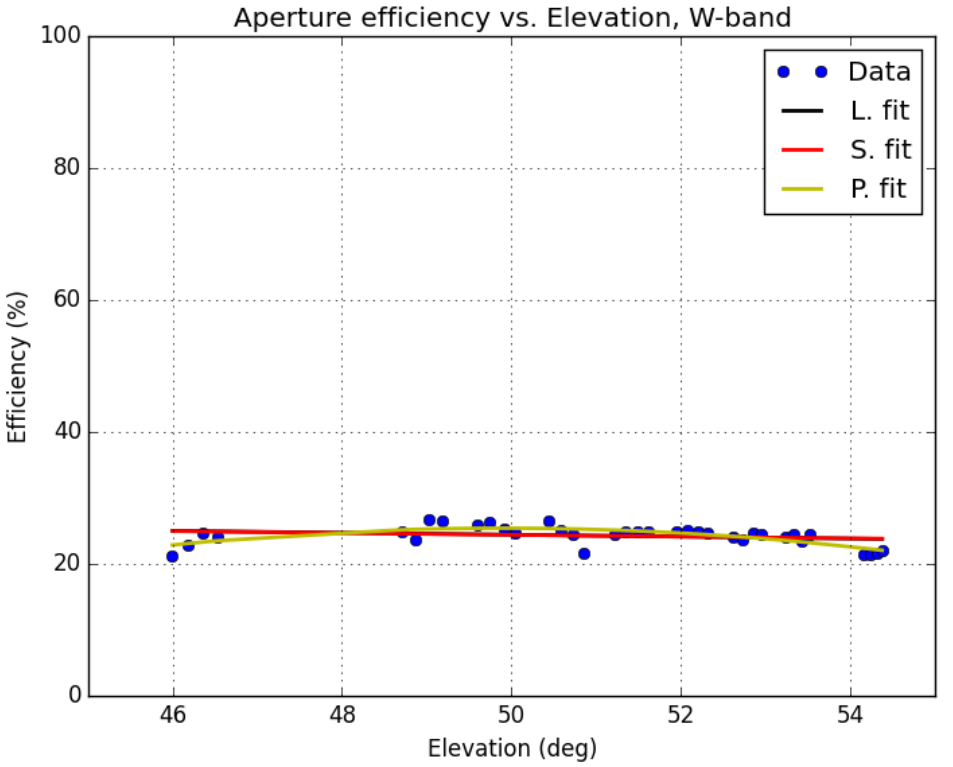

Figure 7: Dependency of the efficiency at W-band on the elevation, together with three fits: linear, sinusoidal and parabollic.

The dependency of the mean aperture efficiency on frequency can be seen in the next figure:

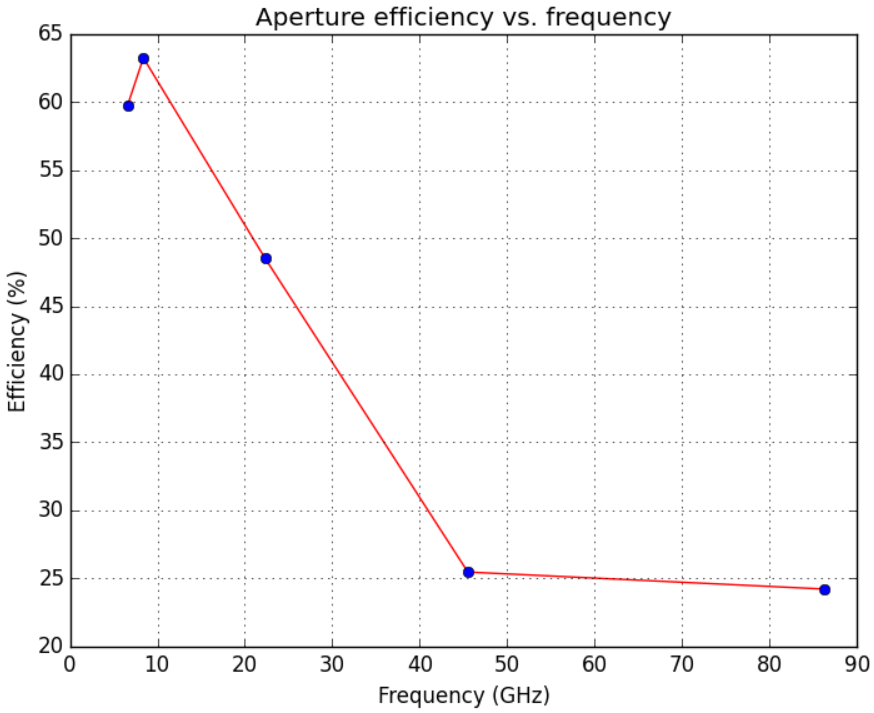

Figure 8: Dependency of the mean efficiency on the observing frequency band.

In the following table the obtained results of aperture efficiency are shown and compared with those tabulated from previous observations in the past:

Band	η_a **mean** (%)	η_a **lin. fit** (%)	η_a **sin. fit** (%)	η_a **par. fit** (%)	η_a **tab** (%)
C	59.77	59.57	59.86	63.86	75.0
X	63.24	67.26	67.61	59.13	70.0
K	48.53	47.36	46.56	43.76	58.0
Q	25.47	25.77	25.89	26.19	45.0
W	24.22	-	-	-	13.0 - 21.0

Table 2: Aperture efficiency values obtained during the current campaign of pointing observations. η_a mean refers to the value calculated by simply taking the mean of the efficiencies obtained for each elevation at each frequency band.

Despite the different fits have also been made for the data from the W-band receiver, the values of η_a derived from them have not been included in the table, since they do not seem to be likely. This can be due the small amount of points considered for the fit, because only a short range of elevations was covered.

Finally, we have calculated as well the *rms* of the random surface errors employing the Ruze's equation,

$$\eta_{M1} = e^{-\left(\frac{4\pi\sigma_s}{\lambda}\right)^2}, \tag{4}$$

and

$$\eta_a = \eta_{M1}\,\eta_{M2}\,\eta_{nm}\,\eta_b\,\eta_{mb}\,\eta_i\,, \tag{5}$$

where η_{nm} includes the efficiencies of the different mirrors on the optical path from the vertex to each receiver in the Nasmyth cabin. In the next table we show the surface efficiency values of the different mirrors:

Mirror	$\sigma_S\,(\mu m)$	$\eta_s(< 22GHz)$	$\eta_s(22GHz)$	$\eta_s(45GHz)$	$\eta_s(86GHz)$	$\eta_s(115GHz)$
M1	194	1.000	0.969	0.875	0.608	0.420
M2	50	1.000	0.998	0.991	0.967	0.944
M3	25	1.000	0.999	0.998	0.992	0.986
M4′	25	1.000	0.999	0.998	0.992	0.986
M5	40	1.000	0.999	0.994	0.979	0.964
M22	40	1.000	0.999	0.994	0.979	0.964
M6	7	1.000	1.000	1.000	0.999	0.999
M7	7	1.000	1.000	1.000	0.999	0.999
M8	17	1.000	1.000	0.999	0.996	0.993
M9	17	1.000	1.000	0.999	0.996	0.993

Table 3: Values of the surface efficiency of the different mirrors in the receivers cabin. σ_S has been calculated employing the Ruze's equation. They have been obtained from http://www.oan.es/rt40m/optica.html .

We have been provided with values of the illumination efficiency, η_i, for each observing frequency [**?**]:

Band	η_i
C	0.66
X	-
K	0.81
Q	0.80 *
W	-

Table 4: Illumination efficiencies at each observing frequency. The value of η_i at Q-band corresponds to a frequency of 43 GHz.

From equations 4 and 5 we have derived the following values of σ_S:

Band	$\sigma_S\,(\mu m)$
C	-
X	-
K	429.17
Q	470.64
W	256.05

Table 5: *rms* calculated from the Ruze's equation and the aperture efficiencies previously obtained.

5 Conclusions

The first and expected result is that the efficiency depends on the frequency (see Fig. 1 and 2). The figures show how efficiency decreases with the frequency as we consider different receivers.

As it can be observed in Fig. 3, 4, 5 and 6, the efficiency curves obtained have a flat tendency overall, but for the case of X-band, where a tendency to decrease at high elevations can be seen. A little distinction between polarizations can also be seen at high elevations for the X-band receiver. The three fits applied seem to be in agreement between them, execpt at high values of elevation for the X-band, again.

Paying attention to dispersion, it appears that at Q-band we have less than at the other frequency bands. This could be due to the fact that less sources were observed at this frequency or maybe the weather conditions were worse at the time the other receivers were employed. In any case, C-band is the one that presents more dispersion.

There is an obvious lost of efficiency in all considered frequency bands but in W-band, though more observations at this band should be carried out. This lost is specially noticeable in C-band and Q-band.

References

[1] Baars, J. W. M. et al. 1977, A&A, 61, 99-106.

[2] de Vicente, P. 2012, IT-OAN 2012-09.

[3] de Vicente, P., Paubert, G., López-Pérez, J.A. et al. 2014, IT-CDT 2014-12.

[4] Fuhrmann, L., Angelakis, E., Zensus, J. A. et al. 2016, A&A, 596, 45.

[5] Perley, R. A. & Butler, B. J. 2016, ApJS.

[6] Tercero, F. 2017, Private communication.

Appendix

A Deconvolution function

The deconvolution function, C_S, has two different forms, depending on the angular size on the sky of the source that is being observed. If we considerer the source to be gaussian, then C_S adopts the form

$$C_S = 1 + x^2 \,, \tag{6}$$

where $x = \theta_S / 1.2\,\theta_b$. On the other hand, if the source is considered to be disky, then the expression for C_S is

$$C_S = \frac{x^2}{1 - e^{-x^2}}\,. \tag{7}$$

The angular size of the source depends on the frequency at which we are observing, and hence we must consider one form of C_S or the other. It is necessary to check the value of the ratio of the angular size of the source to the size of the main beam of the radiotelescope, and then decide which expression to take.

B Source parameters

In the following tables we present the sizes and fluxes used for each source at each observing frequency:

C-band (6.6 GHz)		
Source	**Size** $[''']$	**Flux** $[Jy]$
Tau-A	300.0	505.38
Cas-A	240.0	474.17
Cyg-A	115.0	253.84
Vir-A	200.0	55.68
3C48	1.5	4.24
3C123	23.0	11.82
3C138	0.65	3.15
3C147	1.0	5.86
3C196	6.0	3.05
3C286	1.5	5.96
3C295	5.0	4.47
3C380	1.0	3.60

Table 6: Size and flux of the different sources observed at C-band.

X-band (8.4 GHz)		
Source	**Size** $[''']$	**Flux** $[Jy]$
Tau-A	300.0	454.96
Cas-A	240.0	378.06
Cyg-A	115.0	190.90
Vir-A	200.0	45.23
3C48	1.5	3.32
3C123	23.0	9.37
3C138	0.65	2.66
3C147	1.0	4.71
3C196	6.0	2.37
3C286	1.5	5.08
3C295	5.0	3.36
3C380	1.0	2.63

Table 7: Size and flux of the different sources observed at X-band.

K-band (22.3 GHz)		
Source	**Size** $[''']$	**Flux** $[Jy]$
Venus	24.93	103.46
Saturn	14.42	8.63
DR21	1.0	18.921
3C84	1.0	35.14

Table 8: Size and flux of the different sources observed at K-band.

Q-band (45.5 GHz)		
Source	**Size** $[''']$	**Flux** $[Jy]$
Venus	28.36	432.44
Jupiter	36.3	258.00
Saturn	14.56	36.48
DR21	1.0	14.292
3C84	1.0	27.308

Table 9: Size and flux of the different sources observed at Q-band.

W-band (86.2 GHz)		
Source	**Size** $[''']$	**Flux** $[Jy]$
Venus	56.22	4869.60

Table 10: Size and flux of the different sources observed at W-band.